EasyChair Preprint

№ 5197

LQR and PID Control Design for a Pneumatic Diaphragm Valve

Gerson Conte, Fellipe Garcia Marques and Claudio Garcia

March 23, 2021

LQR and PID Control Design for a Pneumatic Diaphragm Valve

Gerson Yuri Cagnani Conte, Fellipe Garcia Marques, and Claudio Garcia,

***Abstract*—This work demonstrates the design and compares the performance of two different digital control techniques for a modeled pneumatic diaphragm valve. The valve model is derived using first-principles modeling, the Karnopp friction model and approximates the I/P converter dynamics with a first order filter. The digital PID and LQR controllers were chosen to compensate the valve friction. A proposed contribution is to implement a digital LQR control using the Bryson rule and the Pincer technique to tune the matrices Q and R based on requirements response, maximum deviation of states variables and control effort. The robustness of the LQR controller compared to the PID controller is presented in this paper.**

***Keywords*—Digital control, I/P converter, LQR, PID, pneumatic valve.**

I. Introduction

FRICTION is a characteristic of mechanical systems that imposes the biggest challenges during the design of stem position controllers for pneumatic diaphragm valves. The friction index deviation during its life span is common, considering that this phenomenon depends on the maintenance condition of the valve and therefore its wear directly affects it. Since the diaphragm valves are widely employed in the process industry to regulate flow [1], it is important that the position controllers present acceptable performance even when the valve has a high friction index, as sub-optimal control loops may affect the overall plant efficiency.

Oscillations in process variables due to valve stiction, can induce the operator to perform an incorrect controller tuning. In addition, such type of nonlinear oscillations cannot be completely eliminated by controller detuning or by the action of digital valve positioners [2]. Defective or excessively worn valves are responsible for significantly reduce the performance of the plant control loops [3].

The PID is the most commonly used controller to control industrial loops [4]. Its broad adoption can be explained as the PID controller has a simple structure and it is easily understood by the control engineers [5]. Methods to increase the PID tuning performance as Ziegler and Nichols (1942) technique [6] and its variations over the years is still widely used in practice.

The valve friction compensation have been studied [7]. The combinations of control freezing and knocker technique for valve friction compensation can provide good results [8]. However, the Linear Quadratic Regulator (LQR) applied for valve friction compensation is totally new. The LQR design technique is quite studied in modern optimal control theory. One characteristic of the LQR controller is its robustness, which is desirable when designing controllers for models that present uncertainties. For a SISO plant, the LQR has at least a phase margin of 60 degrees and an infinity gain margin [9]. Therefore, the LQR controller is a good choice to study for valve positioners.

The valve that is studied in this paper is an actuator normally used in industrial plants that need flow control in their processes. Pneumatic diaphragm valves are the most fundamental actuators in control applications in chemical engineering plants. Typically, in a single chemical process production unit there can be up to 6000 control valves [10]. However, these actuators may be the ones that present more problems due to high wear and the impact that has been generated by this wear.

II. MODEL

To obtain the valve model, it is possible to apply the balance of forces to the valve stem, according to the Newton's second law, as shown in Equation (1) [10]. The input signal of the valve is defined by the controller (4-20mA), converted into a pressure unit through the I/P converter, and the valve output is the stem position (usually normalized between 0 and 100%). The valve model parameters used in this paper are presented in Table I.

$$m\ddot{x}(t) = F_{diaph} - F_{sp} - F_{at} - F_{flow} - F_{init}, \qquad (1)$$

where m is the moving parts mass (stem + plug + diaphragm), $x(t)$ is the stem position, F_{diaph} is the diaphragm force, F_{sp} is the spring force, F_{flow} is the fluid force that exerts on the valve plug, F_{at} is the friction force, F_{init} is the spring initial force. The diaphragm force and the spring force are presented in Equations (2) and (3).

$$F_{diaph} = S_a p(t), \qquad (2)$$

where S_a is the diaphragm section area and $p(t)$ is the air pressure inside the valve diaphragm chamber and

$$F_{sp} = K_{sp} x(t), \qquad (3)$$

where K_{sp} is the spring constant.

The I/P converter is modeled as a first order filter [11]:

G. Y. C. Conte is with University of Sao Paulo, Sao Paulo, Brazil, e-mail: gerson.cagnani@gmail.com.

F. G. Marques is with Brazilian Navy, Sao Paulo, Brazil, e-mail: fellipegm@gmail.com.

C. Garcia is with University of Sao Paulo, Sao Paulo, Brazil, e-mail: clgarcia@lac.usp.br.

TABLE I
VALVE MODEL PARAMETERS, AS ESTIMATED IN [11].

Variable	Value	Description
$S_a\ (m^2)$	0.0445	diaphragm cross section area
$p_{max}\ (Pa)$	206331	maximum diaphragm pressure
$p_{min}\ (Pa)$	42231	minimum diaphragm pressure
$m\ (Kg)$	1.6	moving parts mass
$K_{sp}\ (N/m)$	206941	spring constant
$F_s\ (N)$	942.4	static friction force
$F_c\ (N)$	665.4	Coulomb friction force
$F_v\ (Ns/m)$	70500	viscous friction force
$F_{init}\ (N)$	2823	spring initial force
$v_s\ (m/s)$	0.00326	Stribeck velocity
$x_{max}\ (m)$	0.02858	maximum stem position
$x_{min}\ (m)$	0	minimum stem position
$K_p\ (Pa/\%)$	1641	pressure gain
$\tau_{I/P}\ (s)$	0.933	time constant of the I/P converter

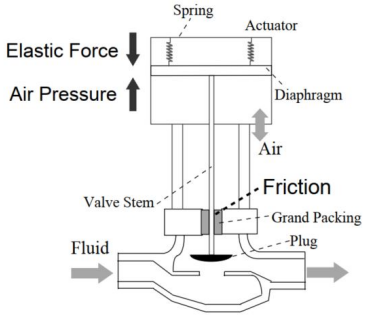

Fig. 1. Simplified schematic of a pneumatic diaphragm valve [1].

$$\dot{p}(t) = \frac{K_p OP(t) + p_{min} - p(t)}{\tau_{I/P}}, \tag{4}$$

where K_p is the pressure gain, $OP(t)$ is the normalized controller output (0 - 100%), p_{min} is the minimum diaphragm pressure and $\tau_{I/P}$ is the time constant of the I/P converter. The pressure gain is defined as:

$$K_p = \frac{p_{max} - p_{min}}{100}, \tag{5}$$

where p_{max} is the maximum diaphragm pressure.

According to [10] the fluid force can be neglected, because it is much smaller than the other forces involved.

A. Friction Models

There are currently several friction models for pneumatic valves, some of them quite simple while others are more sophisticated. Some of these models can be checked at [12]. However, among the main existing models, [13] performed a performance comparison and its conclusion was that the Karnopp [14], LuGre [15] and Kano [1] were able to reproduce the ISA diaphragm valve tests with a high precision.

For this paper, the Karnopp model was selected for the development of controllers and also for the simulations.

B. The Karnopp Friction Model

The Karnopp model describes the friction force F_{at} of Equation (1) establishing the following conditions:

$$F_{at} = \begin{cases} F_{ext}, & if\ |v| < DV\ and\ |F_{ext}| \leq F_s \\ F_s sgn(F_{ext}), & if\ |v| < DV\ and\ |F_{ext}| > F_s, \\ F_d(v), & if\ |v| \geq DV \end{cases} \tag{6}$$

where F_{ext} is the resultant external force, v is the stem velocity, DV is the minimum speed before the stem movement, F_s is the static friction force, $sgn(F_{ext})$ is the sign of F_{ext} quantity and

$$F_d(v) = [F_c + (F_s - F_c)e^{-(v/v_s)^2}]sgn(v) + F_v v, \tag{7}$$

where F_c is the Coulomb friction force, v_s is the Stribeck velocity, F_v is the viscous friction force and $sgn(v)$ is the sign of v.

C. Pneumatic Valve Behavior

It is possible to verify in the previous item that the friction model is discontinuous and non-linear. It can be classified into well known non-linearities, such as *hysteresis*, *dead zone* and *dead band* [16]. Through these characteristics it is possible to obtain some parameters of the valve, for the model of Kano for example. Figure 2 shows what can be called the valve signature [1]. Figure 3 shows the valve signature using the Karnopp friction model.

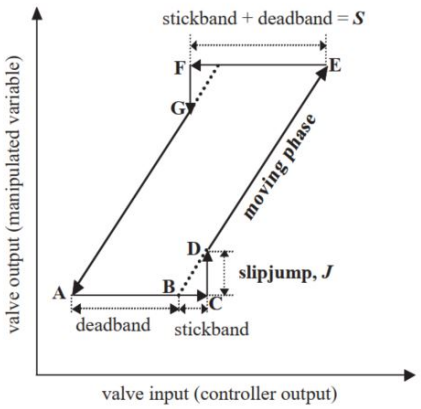

Fig. 2. Typical pneumatic valve signature [17].

The valve stem may become stuck due to a high static friction. This condition can worsen further due to excessive wear and poor maintenance of the valve. During this process, the integrator of the closed-loop controller continues to correct the error, and when the force applied to the stem overcomes the static friction, excessive stem slipping occurs, crossing the desired operating point [17]. Excessive static friction can also reduce the valve operating range.

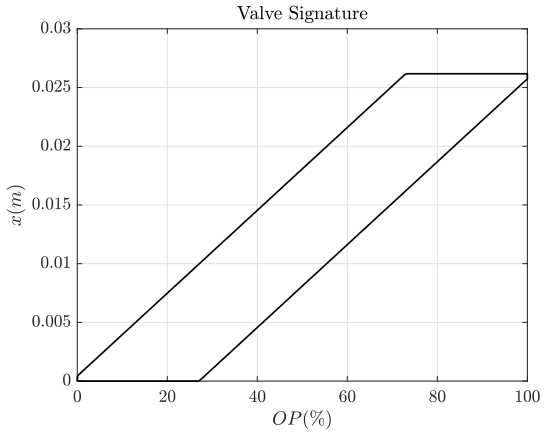

Fig. 3. Algorithm signature of Karnopp friction model.

D. Model Linearization

In order to be able to design the linear controllers, it is necessary to calculate the linear model around the operating velocity. Initially, Equation (1) is expanded in order to separate viscous friction from static friction:

$$\ddot{x} = \frac{S_a K_p}{m} p(t) - \frac{K_{sp}}{m} x(t) - \frac{F_v}{m} \dot{x}(t) - \frac{[F_c + (F_s - F_c) e^{-(\dot{x}(t)/v_s)^2}]}{m} sgn(\dot{x}(t)). \tag{8}$$

Applying the linearization in static friction of Equation (8) around velocity $\dot{x}_L$:

$$\bar{F_{at}}(\dot{x}(t)) = -\frac{2\dot{x}_L}{v_s^2 m}(F_s - F_c) e^{-(\dot{x}_L/v_s)^2} \dot{x}(t). \tag{9}$$

Using a constant C_{ff} to adjust the equation:

$$C_{ff} = -\frac{2\dot{x}_L}{v_s^2 m}(F_s - F_c) e^{-(\dot{x}_L/v_s)^2}. \tag{10}$$

$$\ddot{x} = \frac{S_a K_p}{m} p(t) - \frac{K_{sp}}{m} x(t) - \frac{F_v}{m} \dot{x}(t) + C_{ff} \dot{x}(t) \tag{11}$$

E. The Laplace Transfer Function

According to Equation (11) the Laplace transfer function considering the I/P converter model and the pneumatic valve model is calculated:

$$\frac{X(s)}{U(s)} = \left(\frac{1}{\tau_{I/P} s + 1}\right)\left(\frac{S_a K_p / m}{s^2 + (F_v/m + C_{ff}) s + K_s p/m}\right) \tag{12}$$

The transfer function of the pneumatic valve can be represented as a second order transfer function:

$$G(s) = \frac{\omega_n^2}{s^2 + 2\xi\omega_n s + \omega_n^2} \tag{13}$$

Thus ξ can be calculated as:

$$\xi(\dot{x_L}) = \frac{\frac{F_v}{m} + C_{ff}}{2\sqrt{\frac{K_{sp}}{m}}} \tag{14}$$

The velocity value of the stem was obtained graphically, considering that the behavior of the valve system is underdamped ($0 < \xi < 1$). Therefore, $\xi = 0.5$ was aleatory chosen and for this point, resulted in a linearization point of $\dot{x}_L = 0.001853\, m/s$.

F. State Space Model

The state space model was calculated from Equations (4) and (11):

$$\begin{bmatrix} \dot{p}(t) \\ \dot{x}(t) \\ \ddot{x}(t) \end{bmatrix} = \begin{bmatrix} -\frac{1}{\tau_{I/P}} & 0 & 0 \\ 0 & 0 & 1 \\ \frac{S_a K_p}{m} & -\frac{K_{sp}}{m} & -(\frac{F_v + C_{ff}}{m}) \end{bmatrix} \begin{bmatrix} p(t) \\ x(t) \\ \dot{x}(t) \end{bmatrix} + \begin{bmatrix} \frac{1}{\tau_{I/P}} \\ 0 \\ 0 \end{bmatrix} OP(t)$$

$$y(t) = \begin{bmatrix} 0 & 1 & 0 \end{bmatrix} \begin{bmatrix} p(t) \\ x(t) \\ \dot{x}(t) \end{bmatrix} + \begin{bmatrix} 0 \end{bmatrix} OP(t)$$

III. DIGITAL CONTROLLER DESIGN

For this paper two different techniques design are proposed to perform the closed loop control of the valve. A digital *LQR* and a digital *PID*.

A. Design of Linear Quadratic Regulator (LQR)

The Optimal Quadratic Control is performed by calculating a $\mathbf{K}[n]$ time varying gain. In steady state condition, this gain is constant. It can be obtained in a simpler way than the time variant gain [18]. The K matrix should minimize Equation (15):

$$\mathbf{u}[n] = -\mathbf{K}\mathbf{x}[n]$$

$$J = \frac{1}{2} \sum_{n=0}^{\infty} (\mathbf{x}^T[n]\mathbf{Q}\mathbf{x}[n] + \mathbf{u}^T[n]\mathbf{R}\mathbf{u}[n] + 2\mathbf{x}^T[n]\mathbf{N}\mathbf{u}[u]), \tag{15}$$

Following the system:

$$\mathbf{x}[n+1] = \mathbf{\Phi}\mathbf{x}[n] + \mathbf{\Gamma}\mathbf{u}[n] \tag{16}$$

$$\mathbf{y}[n] = \mathbf{C}\mathbf{x}[n] \tag{17}$$

According to *Bryson Rule* [19] the matrices *Q* (18) and *R* (19) must be diagonal, which are composed of the maximum desired deviations of the states ($Mdxi^2$) and the input ($Mdui^2$).

$$Q_{ii} = \frac{1}{Mdxi^2} \tag{18}$$

$$R_{ii} = \frac{1}{Mdui^2} \tag{19}$$

The *Pincer* technique [20] can introduce another degree of freedom to the LQR controller design, in view of keeping the poles in closed loop within the unit circle of radius $1/\alpha$, with $\alpha > 1$. With that, (15) can be simplified by (20).

$$J = \sum_{n=0}^{\infty} [(\alpha^n \mathbf{x}[n])^T \mathbf{Q} (\alpha^n \mathbf{x}[n]) + (\alpha^n \mathbf{u}[n])^T \mathbf{R} (\alpha^n \mathbf{u}[n])] \tag{20}$$

To calculate the matrix gain K, the *dlqr* command from *MATLAB* © [20] was used.

The *Pincer* technique was used with a criterion of 1%. The calculation of α was performed using Equation (21):

$$\alpha = 100^{\frac{T_s}{t_a}}, \tag{21}$$

where t_a is the settling time and T_s is the controller sampling time [20].

The state space system was expanded with an additional integrator in order to change the regulatory to tracking behavior of the LQR controller. The new structure of Equation (16) is presented in the following matrix:

$$\begin{bmatrix} x[n+1] \\ v[n+1] \end{bmatrix} = \begin{bmatrix} \mathbf{\Phi} - \mathbf{\Gamma} K & \mathbf{\Gamma} K_i \\ -C & I_{mxm} \end{bmatrix} \begin{bmatrix} x[n] \\ v[n] \end{bmatrix} + \begin{bmatrix} 0 \\ I_{mxm} \end{bmatrix} r[n]$$

B. Design of Discretized Positional PID Controller

The PID controller designed for the valve was performed first using the Laplace Transform. It is noteworthy that this controller was designed and implemented in the simulations additionally with the anti-windup function. For that it was considered to assign a zero value for error of the integrative term if $u(t)$ is greater than sat. It also can be done by subtracting from the integative term the error between $u(t)$ and sat multiplied by a gain $1/T_t$, where $T_d \leq T_t \leq T_i$ [21].

A pure derivative term results in a very large amplification of the measurement noise [21], in this case it is possible to approximate this term of the controller according to Equation (22). The complete PID structure is shown in Figure 4.

$$sT_d \cong \frac{sT_d}{1 + sT_d/N}, \tag{22}$$

where T_d is derivative time and N is a gain limitation for high frequencies (usually assigned between 3 to 20) [21].

The method used to discretize the PID controller is the *Rectangular Backwards*. The $u[n]$ output of this digital controller is the sum of the outputs of the controllers: proportional ($u_p[n]$), integral ($u_I[n]$) and derivative ($u_D[n]$). It can be checked in Equation (23).

$$u[n] = u_p[n] + u_I[n] + u_D[n] \tag{23}$$

$$u_p[n] = k_p e[n] \tag{24}$$

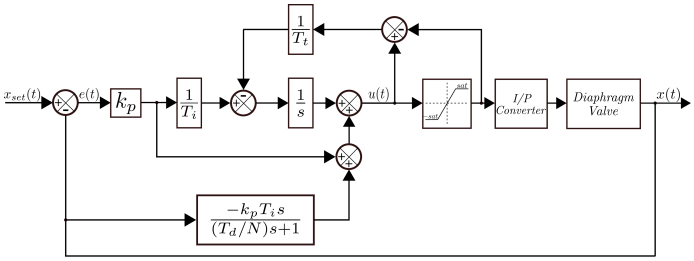

Fig. 4. PID controller with *anti-windup* and *derivative filter*. Adapted from [21].

$$u_I[n] = u_I[n-1] + \frac{k_p T_s}{T_I} e[n] \tag{25}$$

$$u_D[n] = \frac{T_D}{T_D + NT_s} u_D[n-1] - \frac{k_p N T_D}{T_D + NT_s} (y[n] - y[n-1]), \tag{26}$$

where k_p is the controller gain, T_D is the derivative time, T_I is the integrator time, T_s is the sampling time of the controller, N is a gain limitation for high frequencies and $y[n]$ is the system output.

IV. SIMULATION RESULTS

The simulations for controller comparison are performed with Karnopp model non-linearized and with $500Hz$. The controllers are tuned to achieve the maximum values of the requirement response for the linearized Karnopp model in closed loop as follows:

TABLE II
PID PARAMETERS

Overshoot	Settling time	Phase Margin	Gain Margin
10%	$2s$	69°	$43.3dB$

A. PID Tuning and Results

The PID parameters were tuned with the aid of the *Tune* tool, available in the standard *PID* block of *MATLAB*©. The tuned parameters can be verified in Table III. The stem position, stem velocity and control effort of the stem can be verified in Figures 5, 6 and 7, respectively.

TABLE III
PID PARAMETERS

kp	N	T_i	T_d
1.8545	20	0.39364	0.01

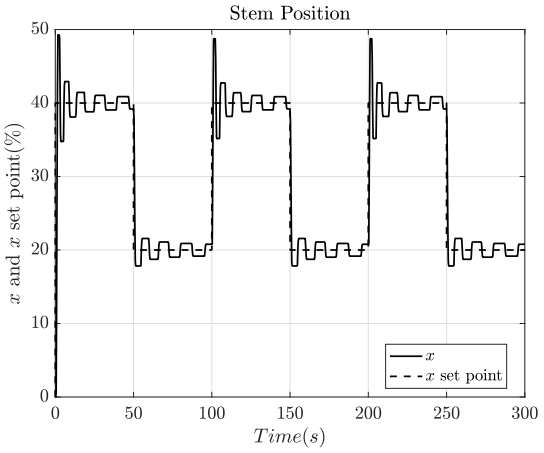

Fig. 5. Stem position for the Karnopp model in closed loop with the PID controller.

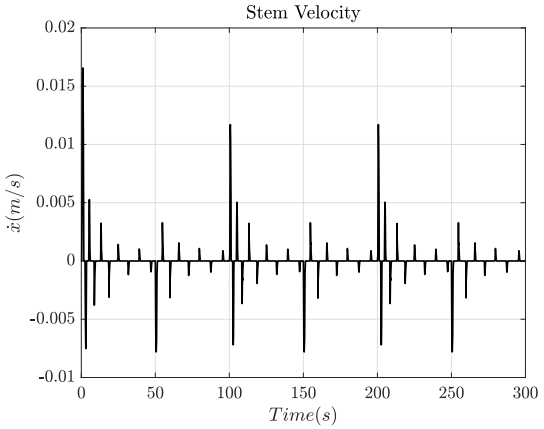

Fig. 6. Stem velocity for the Karnopp model in closed loop with the PID controller.

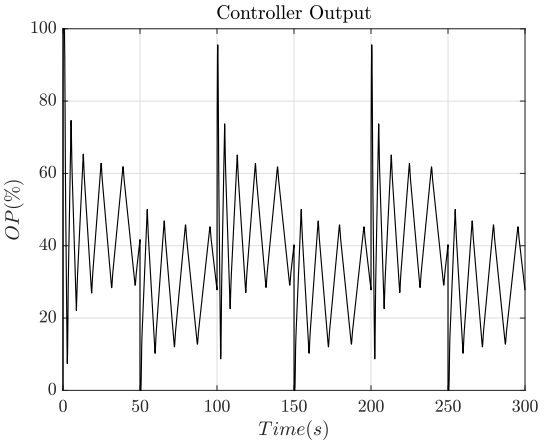

Fig. 7. Control effort of stem for the Karnopp model in closed loop with the PID controller.

B. LQR Tuning and Results

According to the *Bryson Rule*, the maximum desired deviations of the states ($Mdxi^2$) are 1% for the stem position and $2m/s$ for the stem velocity. For integrator state a range between 0 and 100 has been defined and a value of 81.65 was adjusted manually to achieve the maximum deviation values of the other states. For the input ($Mdui^2$), the control effort can be adjusted. This value was adjusted manually with the same purpose of the integrator value. Thus, the **Q** and **R** matrices can be defined as:

$$[Q] = \begin{bmatrix} 0 & 0 & 0 & 0 \\ 0 & \frac{1}{1^2} & 0 & 0 \\ 0 & 0 & \frac{1}{2^2} & 0 \\ 0 & 0 & 0 & \frac{1}{81.65^2} \end{bmatrix}$$

$$[R] = [0.1]$$

The stem position, stem velocity and control effort of the stem can be verified in Figures 8, 9 and 10, respectively.

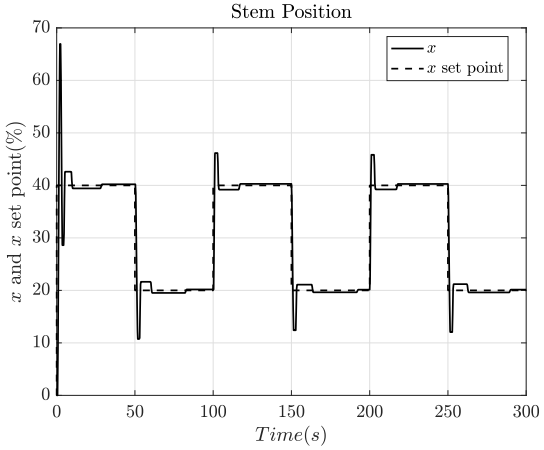

Fig. 8. Stem position for the Karnopp model in closed loop with the LQR controller.

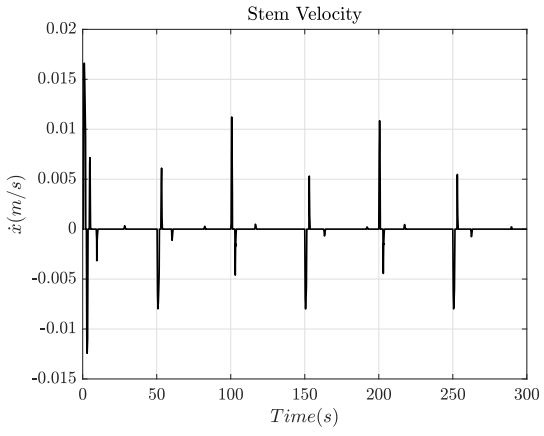

Fig. 9. Stem velocity for the Karnopp model in closed loop with the LQR controller.

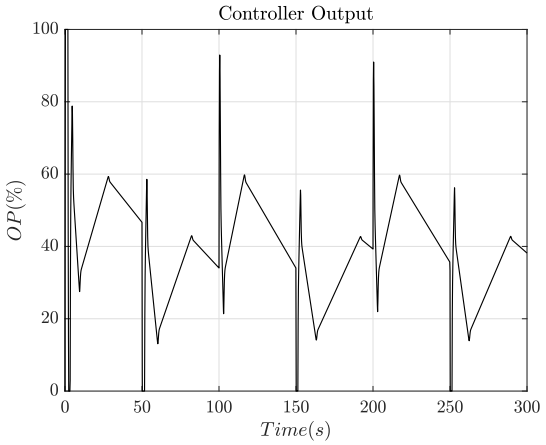

Fig. 10. Control effort of stem for the Karnopp model in closed loop with the LQR controller.

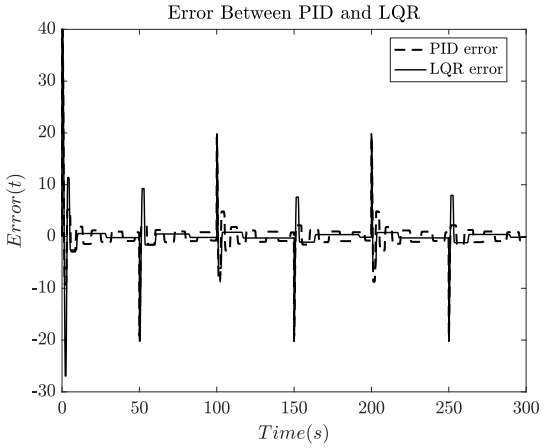

Fig. 11. Error between the PID and LQR controllers.

C. Comparison of PID and LQR Error

The error between the PID and LQR controlles are compared according to three different types of performance indexes: **ISE** *(Integrated Squared Error)*, **VI** *(Variability Index)* and **ITAE** *(Integrated Time-weighted Absolute Error)* considering Equations (27), (28) and (29), respectively. For a fair comparison the first cycle of the response $t < 100$ was discarded, considering that in the first cycle the stem position starts from $x = 0$. The results can be verified in Table IV and Figure 11:

$$ISE = \int_{T_0}^{T} (x - x_{set})^2 dt \tag{27}$$

$$VI = \frac{2\sigma_x}{\mu_x} 100, \tag{28}$$

where σ_x is the standard deviation of the stem position and μ_x is the mean value of the stem position.

$$ITAE = \int_{T_0}^{T} t|x - x_{set}| dt \tag{29}$$

TABLE IV
PERFORMANCE INDEX

Index	PID	LQR
ISE	1300,99	1136,72
VI	14,69	12,13
ITAE	10080,39	4928,57

V. CONCLUSION

The LQR and PID digital controllers were designed and compared. The PID controller presented considerable oscillation and permanent steady state error. It should be noted that the non-linear characteristics of the pneumatic diaphragm valve limit the performance of a linear controller, even with the best tuning. On the other hand, the LQR controller presented better results. It is possible to notice that this controller has a better tracking of the stem position than the PID controller. Other characteristics of the response obtained with the LQR controller should also be highlighted, such as less oscillations and reduced steady state error. The comparison of the performance indexes confirms that. These differences between the responses of the two digital controllers show that, in fact, the LQR controller is more robust than the PID controller. For future work, these controllers are ready to be tested on a real valve.

REFERENCES

[1] M. Kano, H. Maruta, H. Kugemoto, and K. Shimizu, "Practical model and detection algorithm for valve stiction," in *IFAC symposium on dynamics and control of process systems*, 2004, pp. 5–7.

[2] R. B. di Capaci and C. Scali, "Review and comparison of techniques of analysis of valve stiction: From modeling to smart diagnosis," *Chemical Engineering Research and Design*, vol. 130, pp. 230–265, 2018.

[3] M. S. Choudhury, N. F. Thornhill, and S. L. Shah, "A data-driven model for valve stiction," *IFAC Proceedings Volumes*, vol. 37, no. 1, pp. 245–250, 2004.

[4] V. Chopra, S. K. Singla, and L. Dewan, "Comparative analysis of tuning a pid controller using intelligent methods," *Acta Polytechnica Hungarica*, vol. 11, no. 8, pp. 235–249, 2014.

[5] W. L. Luyben, *Process modeling, simulation and control for chemical engineers*. McGraw-Hill, 1996.

[6] J. G. Ziegler, N. B. Nichols *et al.*, "Optimum settings for automatic controllers," *trans. ASME*, vol. 64, no. 11, 1942.

[7] S. Huang, W. Liang, and K. K. Tan, "Intelligent friction compensation: A review," *IEEE/ASME Transactions on Mechatronics*, vol. 24, no. 4, pp. 1763–1774, 2019.

[8] R. Kasikijvorakul and S. Wongsa, "A comparative study on model free valve stiction compensation methods," in *2019 First International Symposium on Instrumentation, Control, Artificial Intelligence, and Robotics (ICA-SYMP)*. IEEE, 2019, pp. 175–178.

[9] J.-B. He, Q.-G. Wang, and T.-H. Lee, "Pi/pid controller tuning via lqr approach," *Chemical Engineering Science*, vol. 55, no. 13, pp. 2429–2439, 2000.

[10] A. Kayihan and F. J. Doyle III, "Friction Compensation for a Process Control Valve," *Control Engineering Practice*, vol. 8, pp. 799–812, 2000.
[11] F. G. Marques and C. Garcia, "Parameter estimation and performance comparison of friction models for pneumatic valves," *Control Engineering Practice*, vol. 104, p. 104629, 2020.
[12] H. Olsson, "Control systems with friction." 1997.
[13] C. Garcia, "Comparison of Friction Models Applied to a Control Valve," *Control Engineering Practice*, vol. 16, no. 10, pp. 1231–1243, 2008.
[14] D. Karnopp, "Computer Simulation of Stick–Slip Friction in Mechanical Dynamic Systems," *Journal of Dynamic Systems, Measurement, and Control*, vol. 107, no. 1, pp. 100–103, 1985.
[15] C. Canudas de Wit, H. Olsson, K. J. Åström, and P. Lischinsky, "A New Model for Control of Systems with Friction," *IEEE Transactions on Automatic Control*, vol. 40, no. 3, pp. 419–425, 1995.
[16] M. A. A. S. Choudhury, M. Jain, and S. L. Shah, "Stiction – Definition, Modelling, Detection and Quantification," *Journal of Process Control*, vol. 18, no. 3–4, pp. 232–243, 2008.
[17] M. A. A. S. Choudhury, N. F. Thornhill, and S. L. Shah, "Modelling Valve Stiction," *Control Engineering Practice*, vol. 13, no. 5, pp. 641–658, 2005.
[18] G. F. Franklin, J. D. Powell, M. L. Workman *et al.*, *Digital control of dynamic systems*. Addison-wesley Reading, MA, 1998, vol. 3.
[19] G. F. Franklin, J. D. Powell, A. Emami-Naeini, and J. D. Powell, *Feedback control of dynamic systems*. Prentice hall Upper Saddle River, 2002, vol. 4.
[20] G. F. Franklin, J. D. Powell, and M. Workman, "Digital control of dynamics," *Ellis-Kagle Press., Half Moon Bay, CA*, 2006.
[21] K. J. Åström and B. Wittenmark, *Computer-controlled systems: theory and design*, 1st ed. Prentice hall Upper Saddle River, 1997.